Small-world Network for Investigating Functional Connectivity in Bipolar Disorder: A Functional Magnetic Images (fMRI) Study

S. Teng[1,2], P.S. Wang[3,4,5], Y.L. Liao[7], T.-C. Yeh[2,6], T.-P. Su[8,9], J.C. Hsieh[2,6], Y.T. Wu[1,2,6]

[1] Department of Biomedical Imaging and Radiological Sciences, National Yang-Ming University, Taipei, Taiwan, ROC
[2] Integrated Brain Research Laboratory, Department of Medical Research and Education, Taipei Veterans General Hospital, Taipei, Taiwan, ROC
[3] The Neurological Institute, Taipei Veterans General Hospital, Taipei, Taiwan, ROC
[4] Department of Neurology, National Yang-Ming University School of Medicine, Taipei, Taiwan, ROC
[5] The Neurological Institute, Taipei Municipal Gan-Dau Hospital, Taipei, Taiwan, ROC
[6] Institute of Brain Science, National Yang-Ming University, Taipei, Taiwan, ROC
[7] National Cheng Kung University, Department of Computer Science and Information Engineering, Taipei, Taiwan, ROC
[8] Division of Psychiatry, School of Medicine, National Yang-Ming University, Taipei, Taiwan
[9] Psychiatric Department, Taipei Veterans General Hospital, Taipei, Taiwan

Abstract — **Small-world network is a highly clustered system but with small mean path length between networks which allow the information transferred with high efficiency. The human brain can be considered as a sparse, complex network modeled by the small-world properties. Once the brain network was disrupted by disease, the small-world properties would be altered to manifest that the information integration was inefficiency and the network was loosely organized. The aim of this study is to investigate the difference of small-world properties of brain functional network derived from resting-state functional magnetic resonance imaging (fMRI) between the healthy subjects and the patients with Bipolar disorder (BD). The functional MRI data was acquired from 5 healthy subjects and 5 patients with Bipolar disorder. All images of each subject were parcellated into 90 cortical and sub-cortical regions which were defined as the nodes of the network. The functional relations between the 90 regions were estimated by the frequency-based mutual information followed by thresholding to construct a set of undirected graphs. Small-world properties, such as the degree and strength of the connectivity, clustering coefficient of connections, mean path length among brain regions, global efficiency and local efficiency, are examined between any pair of functional areas. Our findings indicated that, in comparison with the control subjects, the BD patients presented smaller values of the degree, the strength of the connectivity and the clustering coefficient of connections, whereas larger values of mean path length among brain regions. This suggested the reduced global and local efficiency of the small-world properties for BD patients. In addition, the small-world properties of BD patients were altered significantly in some regions in the frontal lobes and limbic system which were in good agreement with the dysfunction connectivity reported by the previous literatures in the study of bipolar disorder.**

Keywords — **Small-world network, functional connectivity, Bipolar disorder, frequency-based mutual information.**

I. Introduction

A remarkable network between a random network and a regular network is called 'small-word', which is characterized by high cliquishness and short mean path length [1]. The human brain can be considered as a sparse, complex network modeled by the small-world properties, which support rapid integration of information across segregated sensory brain regions, confer resilience against pathological attack, and allow the information transferred between different brain regions with high efficiency. Once the brain network was disrupted by disease, the small-world properties would be altered to manifest that the information integration was inefficiency and the network was loosely organized.

Bipolar disorder (BD) is a category of mood disorders defined by the presence of one or more episodes of abnormally elevated mood. Findings from structural magnetic resonance imaging (MRI) studies suggest that some abnormalities, such as prefrontal sub-region decreased volumes; amygdala and stiatal enlargement and midline cerebellum atrophy. From functional imaging technologies, such as positron emission tomography (PET), single photon emission computed tomography (SPECT) and functional magnetic resonance imaging (fMRI), which are obtained at rest or during cognitive tasks to study specific neural networks, including anterior limbic regions that may underlie bipolar disorder [2,3,4].

These data suggest that activation of 'limbic' prefrontal areas may disrupt of 'cognitive' prefrontal regions. Functional imaging studies support the notion that abnormalities in anterior limbic networks, in which structural and spectroscopic abnormalities have also been reported, appear to underlie the expression of bipolar disorder. The aim of this study is to investigate the difference of small-world properties of brain functional network derived from resting-state

Chwee Teck Lim, James C.H. Goh (Eds.): ICBME 2008, Proceedings 23, pp. 726–729, 2009
www.springerlink.com

functional magnetic resonance imaging between the healthy subjects and the patients with Bipolar disorder.

II. Materials and Methods

A. Data acquisition and preprocessing

The study included 5 patients with bipolar disorder who were recruited from Taipei Veterans General Hospital. Confirmation of the diagnosis for all patients was made by clinical psychiatrists, using the Diagnostic and Statistical Manual of Mental Disorders (DSM). All the five healthy subjects had no history of psychiatric illness. All subjects gave voluntary and informed consent according to the standards set by Taipei Veterans General Hospital.

Imaging was performed on a 1.5 Tesla GE scanner in Taipei Veterans General Hospital. Blood oxygenation level dependent (BOLD) images of the whole brain using an echo planar imaging (EPI) sequence were acquired in 20 axial slices (TR=2000ms, TE=40ms, flip angle=90°, FOV=24cm; 5mm thickness and 1 mm gap). For each subject, the fMRI scanning lasted about 400 seconds. Structural images were obtained using a rapid acquisition gradient echo 3D T1-weighted sequence for each subject (TR=2045ms, TE=9.6ms, flip angle=90°, FOV=24cm). All the preprocessing was carried out using statistical parametric mapping (SPM5). The 200 volumes were first corrected for the acquisition time delay among different slices, and then the all images were realigned to the first volume for head-motion correction. Then, correct differences in image acquisition time between slices. The third step is co-registration: all fMRI images register to the anatomy T1 weighting imaging. The fMRI images were further spatially normalized to the T1 template image.

B. Anatomy parcellation

The registered fMRI data were segmented into 90 regions (45 for each hemisphere, Table1) using the Individual Brain Atlases using Statistical Parametric Mapping Software (IBASPM). For each subject, the representative time series of each individual region was then obtained by simply averaging the fMRI time series over all voxels in this region.

C. Frequency-based mutual information

We applied frequency-based mutual information to each regional time series and estimated the pair-wise inter-regional relations in the specific frequency band (0.01~0.08Hz). We consider the observations of the time series of p points in the brain as finite realizations of a multivariate stationary stochastic process:

$$X(t)=\{X_1(t),X_2(t),...,X_p(t)\},t\in Z \quad (1)$$

We apply the discrete Fourier transform (DFT) to a finite realization of Eq. (1), we have a new set of values

$$Y(\omega_k)=\{Y_1(\omega_k),Y_2(\omega_k),...,Y_p(\omega_k)\} \quad (2)$$

at each $\omega_k(k:1,...,n)$ Fourier frequency. The mutual information between any pair of subsets a, b of Y at frequency ω_k is [5,6]

$$MI_{a,b}(\omega_k)=-1/2\log\left(\left|f_{X_a,X_b}(\omega_k)\right|/\left|f_{X_a}(\omega_k)\right|\left|f_{X_b}(\omega_k)\right|\right) \quad (3)$$

where , $f_{X_a}(\omega_k)$ $f_{X_b}(\omega_k)$and $f_{X_a,X_b}(\omega_k)$are the Hermitian positive definite, (cross-)spectral density matrices of the original processes Xa(t), Xb(t) and {Xa(t), Xb(t)} Symbol $|\ |$ denotes the determinant.

D. Small-world properties

Small-world properties have been described for graphs defined by nodes (brain regions) and undirected edges (functional connectivity). A 90× 90 binary graph can be constructed by applying a threshold T to the frequency-based mutual information. The maximum threshold must assure that each network is fully connected with N= 90 nodes. The minimum threshold must ensure that the brain networks have a lower global efficiency and a larger local efficiency compared to random networks with relatively the same distribution of the degrees of connectivity. The key metrics are the degree and strength of the connectivity, clustering coefficient of connections ,mean path length among brain regions, global efficiency and local efficiency, all defined for each of the i=1,2,3,. . . ,n nodes in the network (Table 1) [7].

Table 1 Small-world indices

Index	Meaning	Formula
K_p	Degree of connectivity	$K_P=\frac{1}{N}\sum_{i\in G}K_i$
E_{corr}	Strength of connectivity	$E_{corr}=\frac{1}{N}\sum_{i\in G}\left(\frac{1}{K_i}\sum_{j\in G_i}\lvert MI(i,j)\rvert\right)$
C_p	Clustering coefficient	$C_P=\frac{1}{N}\sum_{i\in G}\frac{E_i}{K_i(K_i-1)/2}$
L_p	Mean path length	$L_P=\frac{1}{N}\sum_{i\in G}\frac{1}{N-1}\sum_{i\neq j\in G}\min\{L_{i,j}\}$
E_{global}	Global efficiency	$E_{global}=\frac{1}{N(N-1)}\sum_{i\neq j\in G}\frac{1}{L_{i,j}}$
E_{local}	Local efficiency	$E_{local}=\frac{1}{N}\sum_{i\in G}\left(\frac{1}{N_{G_i}(N_{G_i}-1)}\sum_{j,k\in G_i}\frac{1}{L_{j,k}}\right)$

III. Results

The two 90×90 mean functional connectivity matrices shown in Fig.1 were calculated by averaging the frequency-based mutual information matrices of all subjects within the group. The distributions of all the small world properties as a function of threshold from 0.34 to 0.56 within each group are shown in Fig.2. The degree (Kp) evaluates the level of sparseness of a network in Fig.2(A). The strength of the functional connectivity (E_{corr}) of the brain network is shown in Fig.2(B). The cluster coefficient (C_p) measures the extent of a local cluster of the network is shown in Fig2.(C). The mean path length (L_p) measures of the extent of average connectivity of the network is shown in Fig.2(D). The global efficiency (E_{global}) is a measure of the global efficiency of parallel information transfer in the network in Fig.2 (E). The local efficiency (E_{local}) is a measure of the fault tolerance of the network in Fig.2(F). The region analysis for the degree, strength of connectivity, cluster coefficient and mean path length are shown in Fig.3, in which the blue bars and red bars represent healthy subjects and BD patients respectively.

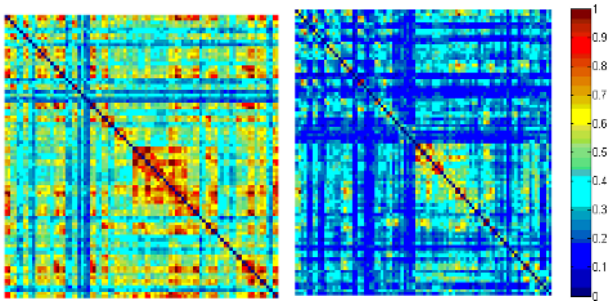

Fig. 1. The mean functional connectivity matrices. Each figure shows 90×90 square matrix, where x and y axes represent the 90 brain regions, and each pixel value indicates the strength of connectivity between each pair of brain regions. The diagonal from upper left to lower right is self-relation, and is set zero. The functional connectivity was stronger in healthy subjects (left) compared with BD patients (right).

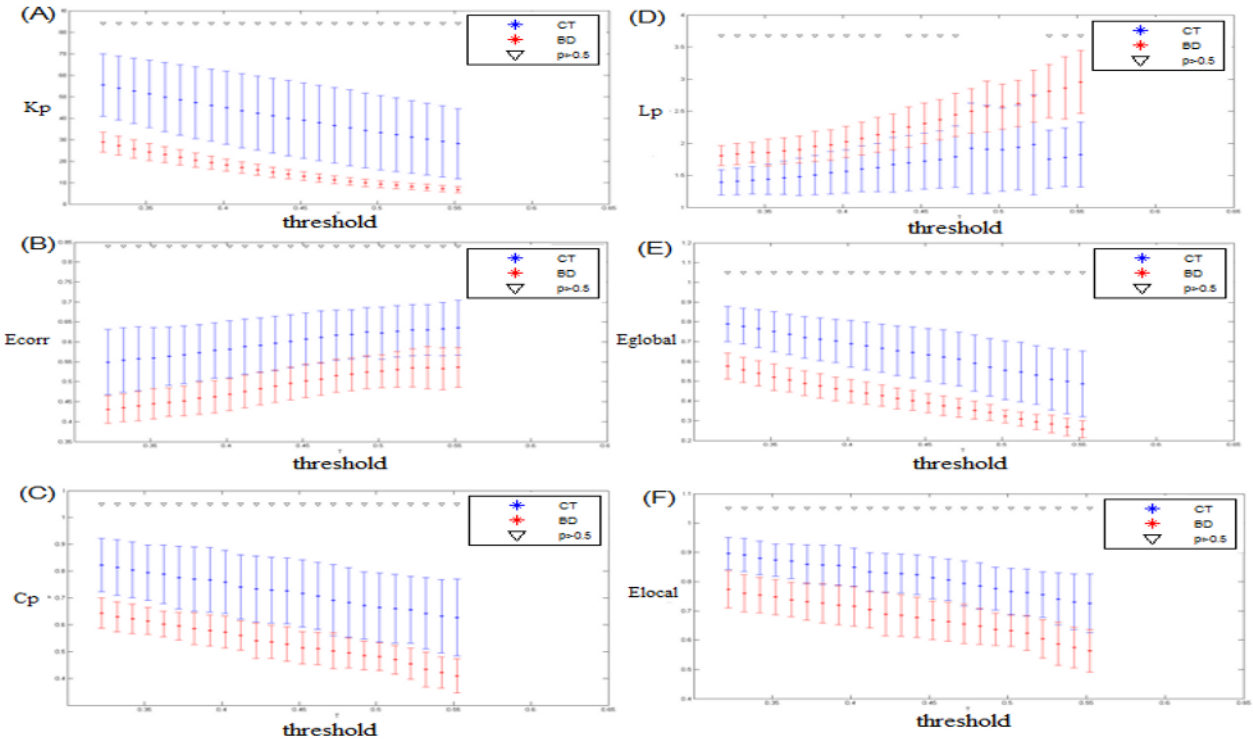

Fig.2. The distributions of all small-world properties. (A) The degree of connectivity (K_p). (B) The strength of connectivity (E_{corr}). (C) The cluster coefficient (C_p). (D) The mean path length (L_p). (E) The global efficiency (E_{global}) (F) The local efficiency (E_{local}). The blue star and red star represent healthy group and BD group, respectively. The black triangle represents the significantly difference between healthy subjects and BD patients.

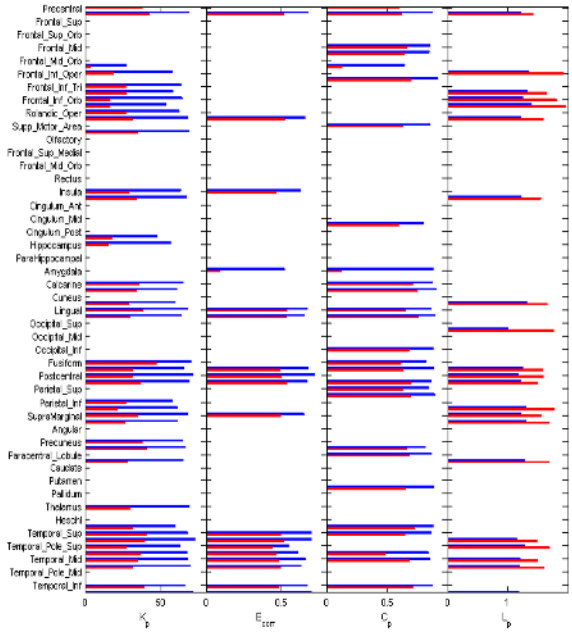

Fig.3 Regional small world properties. The vertical axis is 45 brain regions (both right and left hemispheres), and the horizontal axes are the degree (K_p)., the strength (E_{corr}), the cluster coefficients (C_p) and mean path length (L_p) from left to right in order. Bars indicate the brain region is significantly altered in the relative measurement, and the length of the bar indicates the mean value of the relative measurement between two groups. The blue bars and red bars represent the healthy group and BD group respectively.

IV. Discussion

With an increase in the threshold, the degree (Fig.2(A)) decreases; whereas the strength of the connectivity (Fig.2(B)) increases because increasing the threshold corresponds to eliminate the weaker connections that are more likely to be noisy. Over the whole range of thresholds the degree and strength of connectivity are significantly lower in the BD group. This means the lower connectivity between brain regions in BD patients.

As shown in Fig.2(C) and (D), the higher threshold, the lower cluster coefficient but longer mean path length. The relative lower cliquishness and longer mean path length were presented in BD patients. These results show that the network in BD patients is disrupted.

For all thresholds, both global and local efficiency in Fig.2(E,F) are significantly higher in healthy subjects than BD patients. These results reveal that the information transferred between different brain regions with low efficiency when the brain network was attacked by disease.

We used a two-sample two-tailed t-test to evaluate statistical differences in the four small-world properties between two groups in 90 brain regions at each selected threshold shown in Fig.3. The small-world properties are significantly altered in many brain regions in the frontal, parietal temporal lobes and in limbic system. The similar results in regional analysis show that the brain network in BD patients is sparse and weak connective so that the degree and strength of connectivity are lower. From the lower cliquishness and larger mean path length in BD group indicate the network is loosely organized. Summarize above evidences, the brain network is inefficient in BD patients compared with healthy subjects. Since all thresholds were similar in their trends with respect to the differences in their small-world properties between the BD patients and the healthy subjects, we have chosen to report only one typical threshold (T = 0.34, the top of the threshold range).

V. Conclusion

Our results support the concept that the small-world properties would be altered to manifest that the information integration was inefficiency and the network was loosely organized. These results were in good agreement with the dysfunction connectivity reported by the previous literatures in the study of bipolar disorder. This approach may also be able to be used in other psychiatric disorders such as major depression disease, which can also be taken as a disconnection syndrome and in which abnormal functional connectivity plays a role.

References

1. Duncan J.W. and Steven H.S. (1998) Collective dynamics of small-world' networks. Nature 393:440-442
2. Strakowski S.M., DelBello M.P. and Adler C.M. (2005) The funcitional neuroanatomy of bipolar disorder: a review of neuroimaging findings. Molecular Psychiatry 10: 105-115.
3. Sophia F. (2006) Functional neuroimaging in mood disorders, Phychiatry 5:5.
4. Hilary P.B., Andres M., Joan K. et al. (2003) Frontostriatal abnormalities in adolescents with Bipolar Disorder_Preliminary observations from functional MRI. Am J Psychiatry 106: 1345-1347
5. Salvdor R., Martinez A., Pomarol-Clotet E. et al. (2008) A simple view of the brain through a frequency-specific functional connectivity measure. NeuroImage 39: 279-289
6. Salvador R., Martinez A., Pomarol-Clotet E. et al. (2007) Frequency based mutual information measures between clusters of brain regions in functional magnetic resonance imaging. NeuroImage 35 :83-88
7. Yong L., Meng L., Yuan Z. et al. (2008) Disrupted small-world networks in schizophrenia. Brain 131(4):945-961.

Author: Yu-Te Wu
Institute: Department of Biomedical Imaging and Radiological Sciences, National Yang-Ming University
Street: No.155, Sec.2, Linong Street
City: Taipei
Country: Taiwan, ROCEmail: ytwu@ym.edu.tw